Available online at www.sciencedirect.com
ScienceDirect
Nuclear Physics B 810 [FS] (2009) 491–502
NUCLEAR PHYSICS B
www.elsevier.com/locate/nuclphysb

Simulating the all-order strong coupling expansion I: Ising model demo

Ulli Wolff

Institut für Physik, Humboldt Universität, Newtonstr. 15, 12489 Berlin, Germany

Received 29 August 2008; accepted 24 September 2008

Available online 2 October 2008

Abstract

We investigate in some detail an alternative simulation strategy for lattice field theory based on the so-called worm algorithm introduced by Prokof'ev and Svistunov in 2001. It amounts to stochastically simulating the strong coupling expansion rather than the usual configuration sum. A detailed error analysis and an important generalization of the method are exemplified here in the simple Ising model. It allows for estimates of the two point function where in spite of exponential decay the signal to noise ratio does not degrade at large separation. Critical slowing down is practically absent. In the outlook some thoughts on the general applicability of the method are offered.

1. Introduction

Since about a decade [1] there has been a development in the condensed matter community where a novel approach to the simulation of statistical models was pioneered. One replaces the original partition function given by a sum over certain field configurations by its untruncated series representation, usually the strong coupling or hopping parameter expansion. For any finite but arbitrarily sized system this is regarded as an alternative statistical system that is simulated by a novel Monte Carlo technique. Originally the method has emerged in quantum models that are 'made classical' by using the Trotter formula which leads to world-line type formalisms. In [2] the approach was used for classical spin systems in two and three dimensions.[1] In our opinion this idea is very useful also for investigating systems of interest to lattice field theory

E-mail address: uwolff@physik.hu-berlin.de.

[1] I would like to thank Urs Wenger for drawing my attention to this paper.

0550-3213/$ – see front matter
doi:10.1016/j.nuclphysb.2008.09.033

and elementary particle physics and it might be applicable in suitably generalized form even to fermions and gauge models. Ultimately it could perhaps enable steps toward the long sought generalization of [3] beyond infinite coupling.[2]

In this publication that is planned to be the first of a series, we concentrate our numerical experiments on the 2D Ising model as a prototype system. While the extension to Abelian scalar bosonic theories in any D seems straight-forward—some cases can already be found in [2]—other generalizations will be non-trivial. The purpose of this paper, apart from some reformulation, is on the one hand to introduce an important generalization of biasing the sampling of the series. On the other hand, a more detailed investigation of the behavior of some observables of interest and their comparison with standard methods is made. It should have become clear above that we are not discussing just a new Monte Carlo algorithm but an exact reformulation where physical observables have completely different estimators, variances and autocorrelations which deserve study. Another study of the worm algorithm in the Ising model was recently presented in [4]. There a detailed study of the Monte Carlo dynamics is given refining results in [2]. While we confirm the practical absence of critical slowing down on our lattices, we here do not attempt to determine dynamical critical exponents.

For a first closer look at the method we define

$$Z(u,v)=\sum_{\{s\}} \mathrm{e}^{\beta\sum_{l=\langle xy\rangle} s(x)s(y)} s(u)s(v). \tag{1}$$

Here x, y, u, v denote sites of a cubic periodic lattice in arbitrary dimension D. The outer sum is over Ising configurations $\{s(x)=\pm 1\}$, in the exponent we sum over all links l. This is the numerator of the two point function that may be written as

$$G(x-y)=\big\langle s(x)s(y)\big\rangle=\frac{Z(x,y)}{Z(z,z)}, \tag{2}$$

with an arbitrary lattice site z. Generalizing [2] we consider a new partition function

$$\mathcal{Z}=\sum_{u,v}\rho^{-1}(v-u)Z(u,v). \tag{3}$$

The pairs of sites u, v are now the 'phase space' and $0<\rho(x)<\infty$ is a weight function demanded to possess the lattice periodicity. Constant positive factors in ρ will be irrelevant and we adopt the normalization condition at the origin

$$\rho(0)=1. \tag{4}$$

Now the two point function is given by

$$G(z)=\rho(z)\frac{\langle\langle\delta_{v-u,z}\rangle\rangle}{\langle\langle\delta_{u,v}\rangle\rangle}, \tag{5}$$

where the double bracket $\langle\langle\cdots\rangle\rangle$ denotes averages with respect to (3)

$$\langle\langle A\rangle\rangle=\frac{1}{\mathcal{Z}}\sum_{u,v}A(u,v)\rho^{-1}(v-u)Z(u,v) \tag{6}$$

for observables $A(u,v)$. Note that any dependence of mean values on the weight ρ is canceled in (5), but statistical errors will depend on it.

[2] Similar hopes have been recently expressed by S. Chandrasekharan in his talk at Lattice 2008.

To actually simulate (3) we need $Z(u,v)$ as weights which are not available in closed form. Inserting (1) and enlarging the phase space to $\{u,v,s\}$ would lead to oscillating over-all weights and would not be useful. Instead here the strong coupling expansion may be inserted. In a somewhat sketchy notation, that will become more precise later, we put

$$Z(u,v) = k \sum_{\gamma\in\Gamma(u,v)} (\tanh\beta)^{d(\gamma)}. \tag{7}$$

Here the strong coupling expansion of the Ising model is written in powers of $\tanh\beta$ and k is an unimportant constant. The set of strong coupling graphs contributing to (1) is named $\Gamma(u,v)$ and for each element γ of the set $d(\gamma)$ denotes the degree in $\tanh\beta$ of this contribution. Of course, $\Gamma(u,v)$ includes disconnected graphs that may wind around the torus etc. If we insert this representation into (3) we may consider $\{u,v,\gamma\}$ as phase space points that may now be sampled probabilistically to estimate $\langle\langle\cdots\rangle\rangle$. The very important result of [2] is that it is almost trivial to design an ergodic update from *joint essentially local moves* of $\{u,v,\gamma\}$ under which observables as those appearing in (5) are even (almost) free of critical slowing down. Local here means in particular that in each step γ is deformed only in a minimal way close u or v. A detailed description of the moves will follow. For the graphs of the usual partition function ('vacuum' graphs) alone an ergodic update procedure would be more complicated, it is easier in the enlarged setup. At the same time (5) shows that the extended moves produce information on the two point function if we record the occurring $v-u$ in a histogram.

It may seem surprising that local moves can (almost) eliminate critical slowing down. But this prejudice is of course based on the idea of sampling spin configurations that are long distance correlated. Here as one approaches criticality, bigger strong coupling graphs will be important and apparently the algorithm 'knows' this and may even be guided in addition by choosing ρ appropriately.

There also is an important difference with regard to internal symmetries, the spin flip Z(2) in the Ising case. Spin-flip odd observables cannot be addressed anymore. The contributing graphs reflect the symmetry manifestly and the field variables that transform under the symmetry have been summed over. This should not be seen as a drawback: In the ideal situation of knowing the exact solution this would be the same.

The plan of the paper is as follows. In Section 2 we derive the dimer form of the Ising model that explicitly parametrizes all strong coupling graphs. In addition the update for this system is defined. In Section 3 some numerical results are collected and discussed. We end in Section 4 on conclusions and an outlook, where we offer some speculations on the possibilities to generalize this reformulation and its simulation in various directions.

2. Ising model demonstration

2.1. Dimer formulation

For a single Ising bond the trivial identity

$$\mathrm{e}^{\beta s(x)s(y)} = \cosh\beta \sum_{k=0,1} \big[\tanh(\beta)s(x)s(y)\big]^k \tag{8}$$

holds. Using it on each link with independent dimer or bond variables $\{k_l = 0, 1\}$ we rewrite (1) (up to the factor 2^{-N_x} inserted for convenience) as

$$Z(u, v) = (\cosh\beta)^{N_l} 2^{-N_x} \sum_{\{k,s\}} \prod_l \left[\tanh(\beta) \prod_{x\in\partial l} s(x) \right]^{k_l} s(u)s(v) \tag{9}$$

with the number of links (sites) N_l (N_x). The notation $l = \langle xy\rangle$ has been replaced by the boundary set $\partial l = \{x, y\}$.

Next, the spins are summed over and leave behind the constraint

$$2^{-N_x} \sum_{\{s\}} \prod_l \left[\prod_{x\in\partial l} s(x) \right]^{k_l} s(u)s(v) = \Theta(k; u, v) \in \{0, 1\}. \tag{10}$$

The result Θ factorizes into local constraints with

$$\theta(k; y) = \begin{cases} 1 & \text{if } (\sum_{l,\partial l\ni y} k_l) = \text{even}, \\ 0 & \text{else}, \end{cases} \tag{11}$$

and their complements

$$\bar\theta(k; y) = 1 - \theta(k; y) \tag{12}$$

combining to

$$\Theta(k; u, v) = \left(\prod_{y\notin\{u,v\}} \theta(k; y) \right) \begin{cases} \theta(k; u) & \text{if } u = v, \\ \bar\theta(k; u)\bar\theta(k; v) & \text{else.} \end{cases} \tag{13}$$

In words: If $u = v$ holds, the number of dimers touching at any site has to be even. For $u \neq v$, these two sites have to be surrounded by an odd number of dimers with all other sites being even.

The previous steps coincide with those made in a duality transformation [5]. There, usually with no insertion (or $u = v$), one would solve the constraint by expressing k_l by (the dual of) the discrete 'exterior derivative' [6] of a $D - 2$ 'form' on the dual lattice, yielding self-duality for $D = 2$, the dual gauge theory for $D = 3$, etc. For the algorithm [2], however, we stay with the constrained $\{k_l\}$, in a sense intermediate between the original Ising model and its dual.

The partition function of the enlarged ensemble now reads

$$\mathcal{Z} = \sum_{u,v,\{k_l\}} \frac{\Theta(k; u, v)}{\rho(v - u)} \mathrm{e}^{-\mu\sum_l k_l}, \tag{14}$$

where the dimer sum together with the constraint uniquely label the graphs $\gamma \in \Gamma(u, v)$ and the total dimer number equals $d(\gamma)$. The coupling has been traded for the dimer chemical potential μ,

$$\tanh\beta = \mathrm{e}^{-\mu}. \tag{15}$$

Mean values of observables $A(k; u, v)$, which may now also depend on k_l, are given by

$$\langle\langle A\rangle\rangle = \frac{1}{\mathcal{Z}} \sum_{u,v,\{k_l\}} A(k; u, v) \frac{\Theta(k; u, v)}{\rho(v - u)} \mathrm{e}^{-\mu\sum_l k_l}. \tag{16}$$

Simple diagnostic observables for first Monte Carlo experiments are the internal energy, or equivalently the average nearest neighbor correlation

$$E = \frac{1}{D} \sum_{\nu} G(\hat\nu) \tag{17}$$

and the susceptibility

$$\chi = \sum_z G(z), \tag{18}$$

where we sum over all directions ν and $\hat{\nu}$ are the corresponding unit lattice vectors. The transcription of χ is obvious,

$$\chi^{-1} = \frac{\langle\langle \delta_{u,v} \rangle\rangle}{\langle\langle \rho(v-u) \rangle\rangle}. \tag{19}$$

Thus, in particular for $\rho \equiv 1$, the fraction of coinciding $u = v$ has a simple interpretation and vanishes for $\beta \geqslant \beta_c$ in the thermodynamic limit.

The corresponding translation for E is

$$E = \frac{1}{2D} \frac{\langle\langle \rho(v-u)\delta_{|u-v|,1} \rangle\rangle}{\langle\langle \delta_{u,v} \rangle\rangle}. \tag{20}$$

Alternatively it may be related to the mean dimer occupancy in the subset $u = v$ by differentiating $\ln Z(z,z)$ with respect to β

$$E = \mathrm{e}^{-\mu} + 2\sinh(\mu) \frac{\langle\langle \delta_{u,v} \frac{1}{N_l} \sum_l k_l \rangle\rangle}{\langle\langle \delta_{u,v} \rangle\rangle}. \tag{21}$$

2.2. Prokof'ev–Svistunov worm algorithm

With the algorithm[3] of [2] we sample the ensemble (14). The name of the algorithm presumably derives from the fact that the constraint $\Theta(k;u,v) \neq 0$ requires a line of active dimers ($k_l = 1$) connecting the ends u, v of the worm. However, the connecting sequence of links is not unique, the worm is 'fuzzy' so to speak with fixed head and tail only. We therefore prefer the name PS-algorithm honoring its inventors.

In any case the PS algorithm exploits the fact that we can base an ergodic Monte Carlo algorithm for the ensemble (14) on merely the following two types of simple elementary steps that we apply in alternating order:

- Type I: we pick one of the 2D nearest neighbors of v with equal probability and call it v' and the connecting link l. The proposed move $v \to v'$ with the simultaneous adjustment $k_l \to 1 - k_l$ is accepted with the Metropolis probability

$$p_{\mathrm{acc}} = \min\left(1, \frac{\rho(v-u)}{\rho(v'-u)} \mathrm{e}^{\mu(2k_l-1)}\right), \tag{22}$$

  otherwise the old configuration is maintained. The practical implementation is largely based on precomputed tables. It is not necessary to also move u due to translation invariance.
- Type II: if we encounter a configuration $u, v, \{k_l\}$ with $u = v$ we 'kick' $u = v$ together to a randomly chosen other lattice site with unchanged $\{k_l\}$ with the probability $0 < p_{\mathrm{kick}} < 1$. For $u \neq v$ we do nothing in this step, which is the dominant case.

[3] Originally with $\rho \equiv 1$ only.

Each such I–II step requires $O(1)$ operations, independent of the lattice size. We call this compound a micro-step. For a sequence of $2N_l$ micro-steps ergodicity can be shown. Any two configurations may be connected with non-zero probability by the 'worm dismantling' all active dimers of the first configuration and then 're-building' the second one. The jumps allow to move from one connected component to the next. As usual in ergodicity proofs, this is in general of course a rather academic process! Following [2] we employ $p_{\rm kick} = 1/2$. Some brief numerical experiments with values 0.3 and 0.7 showed that this has hardly any influence. Metropolis acceptance rates in steps I were reasonably far from the extreme values 0 and 1 in all our simulations below, usually between 0.5 and 0.6. In [4] it has been observed that a correct and efficient algorithm can even be based on steps of type I alone ($p_{\rm kick} = 0$) which we have however not tried here.

3. Numerical demonstrations

We group together N_x micro-steps calling this an iteration, during which we accumulate a sub-histogram of occurring separations $v - u$. This may be interpreted as measuring the whole set of 1-bit observables $\{\delta_{v-u,z}\}$—one for each separation z—after each micro-step, mostly implicit zeros, of course. Thus we 'always measure' and never give away any information. Such an iteration has a computational complexity comparable to a sweep in standard algorithms. We separately record the contributions to primary observables from each such iteration. These records are treated as a usual time series and an autocorrelation analysis as described in [7] is made.

Most physically interesting observables are of the derived type, nonlinear functions, typically ratios, of primaries, see (5). Details on their error estimation, including the definition of integrated autocorrelation times for such functions, can also be found in [7]. We only repeat here that in our definition $\sqrt{2\tau_{\rm int}}$ is the ratio between the true and the 'naive' error. Although this is wide-spread, there are alternative definitions in the literature that may coincide with this one only for large $\tau_{\rm int}$, a case not relevant here.

The tests below are in $D = 2$ using lattices of size $T \times L$, but they are expected to be representative for larger D, too.

3.1. Simulations at β_c with $\rho \equiv 1$

Results for χ in the form (19) and E from both (20) and (21) are reported. For each lattice size we have performed 10^6 iterations after equilibration.[4] The values are compatible, for instance, with [8] and our results with integrated autocorrelation times are listed in Table 1. We confirm the practically complete absence of critical slowing down for the observables under study.

It is instructive to compare the achieved precision with that of the single cluster simulations in combination with standard spin estimators that were reported in [8]. The energy E is a useful monitor for simulations but non-universal and not really of physical interest. We hence concentrate on χ which contains long distance contributions. We first compare the growth of $\tau_{{\rm int},\chi}$ here with the one quoted in [8] for the single cluster (1C) algorithm. While both algorithms are very fast, the PS simulations seem to have even smaller and less rising $\tau_{{\rm int},\chi}$. Does this automatically mean that PS is preferable for measuring χ? As we estimate in a completely different ensemble also the variance can be quite different. In [8] errors are quoted for χ together with the number

[4] Here and below we generously spend 10% of the total statistics for equilibration.

Table 1
Values and integrated autocorrelation times for simulations at the critical point $\beta = \ln(1+\sqrt{2})/2$ and various lattice sizes.

$T = L$	$L^{7/4}/\chi$	$\tau_{\mathrm{int},\chi}$	E (20)	$\tau_{\mathrm{int},E}$ (20)	E (21)	$\tau_{\mathrm{int},E}$ (21)
16	0.9166(28)	0.813(14)	0.7263(10)	0.567(5)	0.7267(5)	1.94(4)
32	0.9153(33)	0.815(14)	0.7171(9)	0.535(6)	0.7171(3)	2.13(4)
64	0.9117(38)	0.860(15)	0.7116(8)	0.517(5)	0.7120(2)	2.41(5)
128	0.9196(44)	0.928(17)	0.7096(7)	0.508(3)	0.7097(1)	2.60(6)
256	0.9102(49)	0.933(17)	0.7089(7)	0.504(3)	0.7083(1)	2.81(7)

of single cluster steps performed. Using the average cluster size (that actually equals χ) it is an easy exercise to predict the errors for a single cluster run of 10^6 steps per spin, a CPU effort similar to the one in this study. Taking $L = 256$ as an example, the result is that the error on χ from a single cluster simulation would be about 6 times smaller.

Due to the simplicity of the estimator (19) we immediately know the variance

$$v_{\chi^{-1},\mathrm{PS}} = \left\langle\!\left\langle \left(\delta_{u,v} - \chi^{-1}\right)^2 \right\rangle\!\right\rangle = \chi^{-1} - \chi^{-2} \approx \chi^{-1}. \tag{23}$$

Given the known final errors and the fact that we effectively measure after each micro-step, we can also conclude the integrated autocorrelation time $\bar{\tau}_{\mathrm{int},\chi}$ in time units of micro-steps. It ranges from about $\bar{\tau}_{\mathrm{int},\chi} \approx 9$ for $L = 16$ to $\bar{\tau}_{\mathrm{int},\chi} \approx 53$ for $L = 256$. This means that an effectively independent estimate for χ^{-1} arises after moving dimers (modifying the strong coupling graphs) in only a small part of the volume. The point is that we are discussing an *integrated* autocorrelation time and not *the slowest mode*. Our observable couples, for instance, only weekly to remote parts of the graph. Nevertheless, as discussed above, taking into account also the variance, no miracle in terms of efficiency has happened! In [4] quite similar observations have been made for χ. In their comparison with the Swendsen–Wang cluster algorithm PS fares however somewhat better.

We end this subsection by visualizing a typical contributing graph in Fig. 1.

3.2. Biased PS: Making use of ρ

One use of the generalization of arbitrarily biasing the ensemble (14) with $\rho \not\equiv 1$ may be seen as follows. We assume to be able to guess an approximate form of the two point function (up to a factor) and use this for ρ. Then (5) shows that the Monte Carlo produces an approximately z-independent correction factor that turns our guess into the exact correlation. This means, up to fluctuations and imperfections of our guess, all our counting-bins of occurring $v - u$ will have approximately equal filling. Apart from autocorrelation effects—which will be found to be minor—this means that the *relative* statistical error of correlations measured in this way will be $c/\sqrt{N}$ with the number of iterations N and essentially the same constant c for all separations. This implies a constant signal to noise ratio independent of the size of the signal, a rather unusual situation.

We first tested this mechanism in the critical model simulated before. The actual method to set ρ was: In a first simulation with $\rho = 1$ where we spent about 10% of the planned total statistics, we have measured G after some equilibration. Although not mandatory, we symmetrized the observed histogram 'by hand' over the geometric lattice symmetries: reflections along the two directions and, if $T = L$ holds, cubic rotations. These symmetries were, of course, only violated

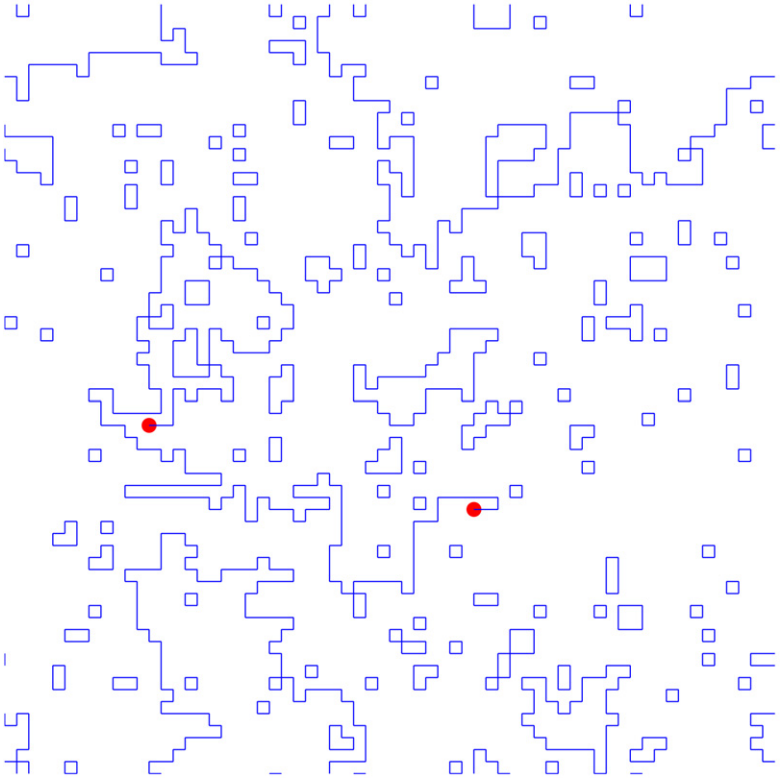

Fig. 1. A typical contribution for $T = L = 64$, $\beta = \beta_c$ without bias, $\rho \equiv 1$. The blobs are at u and v, lines show $k_l = 1$.

by the statistical fluctuations. With this ρ we then performed the main simulation.[5] We have indeed observed almost flat $\langle\langle \delta_{v-u,z} \rangle\rangle$ and compatibility with the known results. Nevertheless there is no significant gain in precision which was not unexpected: At criticality, in a finite volume, the two point function does not decay exponentially but only by relatively moderate factors. The real strength of the possibility of biasing toward larger separations is expected in the massive disordered phase $\beta < \beta_c$ which we study next.

3.3. Mass gap in the disordered phase

In many applications one is interested in low-lying eigenvalues of the transfer matrix. We pick a Euclidean time direction and resolve the lattice site label into two-vectors $x = (x_0, x_1)$ labeling sites on a $T \times L$ torus and work in lattice units, $a = 1$ (integer x_ν). We want to study the temporal decay of correlations at fixed spatial momentum p_1

$$G_{p_1}(x_0) = \sum_{x_1} G(x_0, x_1) \mathrm{e}^{-ip_1 x_1}. \tag{24}$$

[5] In more difficult cases one could think of a sequence of improving approximations.

It is not difficult to see that in the dimer representation it is given by

$$G_{p_1}(t) = \frac{\langle\langle \rho(t, v_1 - u_1)\delta_{v_0-u_0,t} \mathrm{e}^{-ip_1(v_1-u_1)}\rangle\rangle}{\langle\langle \delta_{u,v}\rangle\rangle}. \tag{25}$$

In the present study we restrict ourselves to observing the mass gap and probe with $p_1 = 0$ only. Moreover, we found by a short test that for this observable there is no disadvantage in letting ρ only depend on time. Then the correlation simplifies to

$$G_0(t) = \rho(t)\frac{\langle\langle \delta_{v_0-u_0,t}\rangle\rangle}{\langle\langle \delta_{u,v}\rangle\rangle}. \tag{26}$$

We now need a guess of the time-slice correlation and use this for ρ and have the Monte Carlo again only work out the corrections. It is sufficient to histogram only the time separations and in addition count coincidences $u = v$, if the normalization is needed. Due to symmetry we may combine t and $T - t$.

Below, instead of showing the correlation itself, we shall consider the time dependent effective mass. Taking care of time periodicity we define $m(t + 1/2)$ by numerically solving for m in

$$\frac{G_0(t+1)}{G_0(t)} = \frac{\cosh(m(T/2 - t - 1))}{\cosh(m(T/2 - t))}, \quad m > 0, \quad 0 \leqslant t < T/2, \tag{27}$$

which for $mt \gg 1$ is expected to plateau at the asymptotic mass-gap of the transfer matrix. This finite volume mass gap has a weak L-dependence and approaches the true gap for large mL. Here we are not interested in this second limit but just work around $mL \approx 5$ and below β_c.

For a test-bed with $L = 64$, $T = 256$, $\beta = 0.42$ we show in Fig. 2 the effective mass from several simulations. The horizontal lines are the exactly known result[6] from [9]

$$m_{\mathrm{ex}}[L = 64, \beta = 0.42] = 0.0841370\ldots. \tag{28}$$

Each of the plots corresponds to 10^6 steps per lattice site. The uppermost panel shows the standard situation in a favorable case. We have carried out 10^6 sweeps of the Swendsen–Wang algorithm and have measured the standard spin-estimator. Due to our large statistics and a well isolated spectrum, we see a clear plateau forming *before* the errors explode at larger separation. As usual in such estimations, while the signal G_0 vanishes exponentially the variance remains essentially constant. This could in principle be improved by cluster estimators, but the signal to noise ratio would still vanish exponentially with t, only at a slower rate.

In the next panel from above we see the result of a PS simulation with $\rho \equiv 1$. The general impression is similar as before. The errors are somewhat larger at small t and smaller at large t. For the next simulation we have biased for a flat histogram using an analytical guess $\rho \propto \cosh(m(T/2 - t))$ with a mass close to the expected one. We are rewarded with a completely uniform error independent of t. In additional experiments we tried to over-sample long distances and have used

$$\rho \propto \cosh\big[(m + 2n/T)(T/2 - t)\big], \tag{29}$$

which exponentially favors $v_0 - u_0 = T/2$ over $v_0 = u_0$ by a factor $\exp(n)$. The bottom plot in Fig. 2 shows the case $n = 3$. We indeed see even smaller errors at large t (about a factor 0.6)

[6] I would like to thank Martin Hasenbusch for advise with the Ising literature and for a C-code that evaluates the finite volume mass-gap.

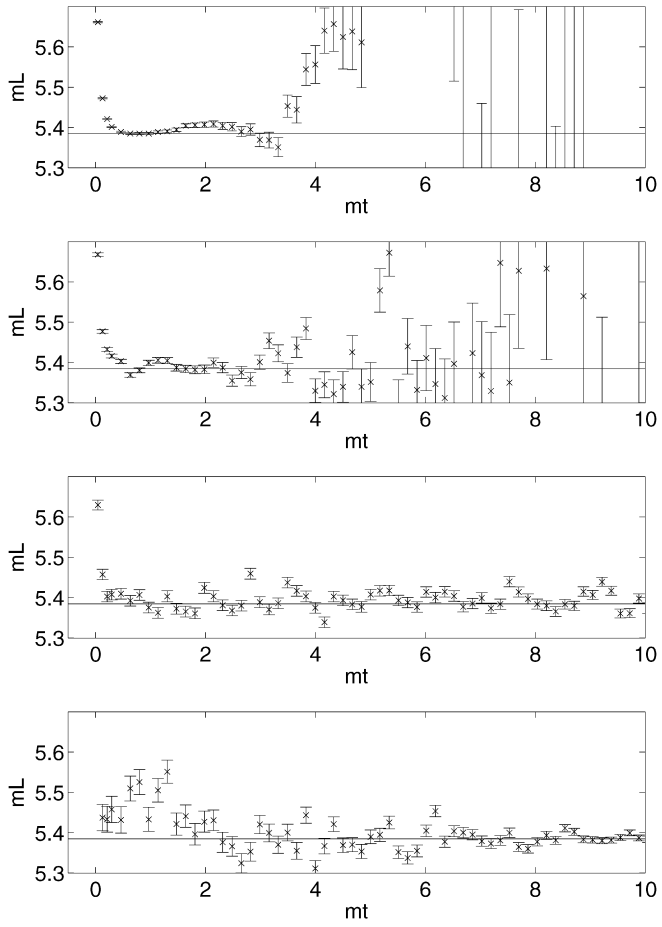

Fig. 2. Plots of the effective mass (times L) versus separation t in correlation length units. From top to bottom: standard spin simulation, $\rho \equiv 1$, $\rho = \cosh(m(T/2-t))$, $\rho = \cosh((m+6/T)(T/2-t))$. Errorbars are one sigma.

where systematic errors are smallest, a reversal of the standard situation where one usually has to compromise between systematics and statistics. The three PS runs took equal CPU time and the cluster simulation in our implementation was a factor two longer, all on a single PC.

For extremely non-uniform choices of ρ we expect to eventually run into a problem, because u, v have to travel over the whole lattice including all separations for ergodicity. If one approaches such a case gradually, as we did varying n, this should not set in abruptly but autocorrelation times should start to rise. For the case above, and even for $n > 3$, we have hardly seen such effects except that sometimes the summation window [7] for the autocorrelation function, in particular for E, had to be increased to capture its tail. All observed integrated autocorrelation times of effective masses were very close to $1/2$ in units of iterations. In addition we notice that in the PS data the errorbars jump around the exact line while the spin simulation results exhibit longer wavy structures. This indicates that the PS data from different time separations are statistically less dependent. Averaging the effective mass over a range or performing a fit in some suitable window would probably reduce the error significantly. If we take the deviations from the

known constant for say $mt > 2$ and the determined errors to form a χ^2-value, we find reasonable values close to the number of data points entering. We do however not attempt to optimize the mass gap extraction any further here in this demonstration of principles.

4. Conclusions and outlook

We have investigated the worm algorithm of Prokof'ev and Svistunov in the case of the tanh β expansion of the Ising model. We emphasize that this involves a reformulation of the problem as a different statistical sum rather than just a new simulation algorithm to produce thermalized spin configurations. We confirm [2] and [4] to the effect that critical slowing down in practice is no issue for this method, at least in the case studied here. The important generalization of biased sampling ($\rho \not\equiv 1$) allowed us to estimate the two point function in the disordered massive phase with a signal to noise ratio that does not decay with distance. Even the contrary can be achieved.

We expect that these features immediately generalize to other scalar models with Abelian field variables, e.g. ϕ^4, Z(N) clock models, U(1) XY-model, Potts models in arbitrary dimension. A high precision study using the PS algorithm for the phenomenologically important XY model in $D = 3$ was already presented in [10]. In [11] the elimination of the sign-problem for bosons in a non-vanishing chemical potential by the PS-method is demonstrated. For correlations beyond two point functions one could consider more insertion points, perhaps with partially restricted domains. For non-Abelian spin models like O(N), RP(N), CP(N), SU(N) $\times$ SU(N) the expansion and constraints are clearly more involved but hopefully still manageable. It should perhaps be kept in mind that for the continuum limit one is not confined to the standard actions of these models. An immediate generalization will be the world-line or loop-gas formulation of lattice fermions as presented in [12]. A similar representation can be written for fermions in more than two dimensions. It will be all decisive for the future usefulness of the approach whether the sign-problem can be handled there. In two dimensions it is essentially absent and successful worm simulations have in fact already been reported [13]. This will allow for the simulation of the O(N)-invariant Gross–Neveu model where along the lines of [12] we have encountered some problems with the measurement of interesting correlation functions. Another important generalization would be lattice gauge theory. There the insertion of spin fields obviously should be generalized to Wilson loop insertions and gauge invariance will be manifest term by term. In this way it will hopefully be possible to efficiently generate the strong coupling graphs. The closed surfaces of the vacuum graphs will be embedded in a larger class of graphs with surfaces with boundaries as discussed to some degree in [11]. Also here the Abelian case will be much simpler than for example SU(2). First efforts towards a non-Abelian dual formulation (without so far employing a PS-type algorithm) can be found in [14]. The ultimate dream, of course, would be an efficient alternative simulation technique for full QCD.

Acknowledgements

I would like to thank Willi Rath and Urs Wenger for discussions and Oliver Bär in addition also for useful comments on the manuscript. Support by the Deutsche Forschungsgemeinschaft (DFG) in the framework of SFB Transregio 9 is acknowledged.

References

[1] N.V. Prokof'ev, B.V. Svistunov, I.S. Tupitsyn, "Worm" algorithm in quantum Monte Carlo simulations, Phys. Lett. A 238 (1998) 253.

[2] N. Prokof'ev, B. Svistunov, Worm algorithms for classical statistical models, Phys. Rev. Lett. 87 (16) (2001) 160601.
[3] P. Rossi, U. Wolff, Lattice QCD with fermions at strong coupling: A dimer system, Nucl. Phys. B 248 (1984) 105.
[4] Y. Deng, T.M. Garoni, A.D. Sokal, Dynamic critical behavior of the worm algorithm for the Ising model, Phys. Rev. Lett. 99 (2007) 110601.
[5] F.J. Wegner, Duality in generalized Ising models and phase transitions without local order parameters, J. Math. Phys. 12 (1971) 2259–2272.
[6] K. Drühl, H. Wagner, Algebraic formulation of duality transformations for Abelian lattice models, Ann. Phys. 141 (1982) 225.
[7] U. Wolff, Monte Carlo errors with less errors, Comput. Phys. Commun. 156 (2004) 143–153.
[8] U. Wolff, Comparison between cluster Monte Carlo algorithms in the Ising model, Phys. Lett. B 228 (1989) 379.
[9] B. Kaufman, Crystal statistics. 2. Partition function evaluated by spinor analysis, Phys. Rev. 76 (1949) 1232–1243.
[10] E. Burovski, J. Machta, N. Prokof'ev, B. Svistunov, High-precision measurement of the thermal exponent for the three-dimensional XY universality class, Phys. Rev. B: Condens. Matter Mater. Phys. 74 (13) (2006) 132502.
[11] M.G. Endres, Method for simulating $O(N)$ lattice models at finite density, Phys. Rev. D: Part. Fields Gravit. Cosmol. 75 (6) (2007) 065012.
[12] U. Wolff, Cluster simulation of relativistic fermions in two space–time dimensions, Nucl. Phys. B 789 (2008) 258–276.
[13] U. Wenger, LEILAT08 workshop, Leipzig, June 2008, and private communication.
[14] J.W. Cherrington, A dual algorithm for non-Abelian Yang–Mills coupled to dynamical fermions, Nucl. Phys. B 794 (2008) 195–215.